AIMS Mathematics, 10(4): 9516–9538.
DOI: 10.3934/math.2025439
Received: 13 February 2025
Revised: 08 April 2025
Accepted: 15 April 2025
Published: 25 April 2025

https://www.aimspress.com/journal/Math

Research article

Bifurcation and chaos analysis of the Kadomtsev Petviashvili-modified equal width equation using a novel analytical method: describing ocean waves

Amna Mumtaz[1,†], Muhammad Shakeel[1], Abdul Manan[2], Marouan Kouki[3,*] and Nehad Ali Shah[4,†,*]

[1] Department of Mathematics, Faculty of Basic Sciences, University of Wah, Wah Cantt 47040, Pakistan; amna.mumtazsyed@gmail.com, muhammad.shakeel@uow.edu.pk
[2] Department of Mathematics, Faculty of Sciences, Superior University, Main Campus Lahore, Pakistan; abdul.manan@superior.edu.pk
[3] Department of Information System, Faculty of Computing and Information Technology, Northern Border University, Rafha, Saudi Arabia
[4] Department of Mechanical Engineering, Sejong University, Seoul 05006, Republic of Korea

[†] These authors contributed equally to this work and are co-first authors.

*** Corresponding:** Email: marouan.kouki@nbu.edu.sa, nehadali199@yahoo.com.

Abstract: This work investigated the Kadomtsev Petviashvili-modified equal width (KP-mEW) equation describing ocean waves. Our focus was on the analysis of the KP-mEW equation from various angles, including the study of soliton solutions, bifurcation analysis, multistability, and Lyapunov exponents. First, a transformation was used to transform the partial differential equation (PDE) into an ordinary differential equation (ODE), from which the soliton solutions were obtained by using a new modified (G'/G^2)-expansion method. We investigated different types of solutions of the KP-mEW equation with various parameters, including kink, periodic, singular periodic, singular kink, and singular periodic-kink solutions. We also simulated 3D and 2D plots for some solutions to enhance the visualizations. These graphical representations provide important information about the patterns and dynamics of the solutions, leading to a strong understanding of the behavior and applicability of the model. We also observed the chaotic behavior of the system by adding a perturbation term and analyzed the chaotic behavior through bifurcation plots, multistability and time series analysis, and Lyapunov

exponents and obtained various dynamic modes such as periodic and quasi-periodic types. A comparison of the obtained solutions with the existing solutions was also presented in the form of Table 1.

Keywords: new modified (G'/G^2)-expansion method; nonlinear KP-mEW equation; traveling wave solution; exact solutions; soliton solutions; chaotic analysis
Mathematics Subject Classification: 34G20, 35A20, 35C07, 35C08

1. Introduction

Nonlinear models effectively explain complex natural phenomena in several areas. Recent advances in mathematics and physics have greatly expanded our understanding of these systems [1]. Ma and Geng [2] proposed a new coupled nonlinear Schrödinger type equation, and obtained several explicit analytical solutions, including periodic and rational solutions by using Darboux transformation. Yong et al. [3] conducted analysis of the singularity structure of the new nonlinear Schrödinger type equation and created several explicit wave solutions by performing direct quadrature and Painlevé expansion approaches. Innovative and broad closed form traveling wave solutions in terms of hyperbolic, trigonometric and rational were obtained by Akbar et al. [4] by using the rational (G'/G)-expansion method of three nonlinear partial differential equations. The extended (G'/G), semi-inverse, and sine-cosine techniques were used by Kopcasiz et al. [5], and obtained bright, bright-dark, dark, periodic, combined singular soliton, rational and solitary wave solutions of nonlinear Schrödinger equation. Closed-form solutions in terms of hyperbolic, trigonometric, and rational function solutions of the simplified modified Camassa-Holm equation were obtained by Shakeel et al. [6] by using the novel (G'/G^2)-expansion scheme. Such models now represent the precise process of population dynamics through optical fibers, fluid dynamics, plasma physics, and wave solutions. Researchers are scrutinizing these nonlinear systems using both numerical and analytical approaches.

Some methods have been proposed such as the modified exp-function method [7], exp function method [8], extended exp-function method [9], modified F-expansion [10], tanh-function method [11], modified Sardar sub-equation method [12], Kudryashov method [13], improved $\tan(\phi/2)$-expansion [14], sine-cosine functions [15], first integral scheme [16], the simplest equation method and its modification [17,18], modified reduced differential transform method [19], modified simple equation method [20], and generalized auxiliary equation approach [21].

In this work, a recently developed technique, the novel modified (G'/G^2)-expansion method as validated in [22], is used to obtain new wave solutions for the KP-mEW equation. The KP-mEW equation is the result of combining the Kadomtsev Petviashvili (KP) equation with the mEW equation, where it has the following form:

$$\left(u_t + a(u^3)_x + bu_{xxt}\right)_x + ru_{yy} = 0. \tag{1.1}$$

This interesting model is obtained by Wazwaz [15]. The cubic nonlinear mEW equation associated with the nonlinear transient wave solution is given as below [23,24]:

$$u_t + 3u^2u_x - \kappa u_{xxt} = 0. \tag{1.2}$$

Equation (1.2) is related to the regularized nonlinear long wave equation having solitary waves including altering amplitude of uniform width. Also, the KP equation demonstrating the nonlinear oscillatory behavior of waves is as follows:

$$\left(u_t + auu_x + u_{xxx}\right)_x + u_{yy} = 0. \tag{1.3}$$

Equation (1.1) has an important practical application of equations that have been modified to the same width (KP-mEW) equation, particularly in the modeling of nonlinear wave phenomena in various scientific fields. Marine engineering describes the spread and interactions of long waves such as tsunamis and tide drilling that support coastal protection and disaster prediction. In plasma physics, this equation is useful for the analysis of ionic acoustic waves and lonely dynamics. This is extremely important for merged energy research and space plasma research. Furthermore, it plays a role in the nonlinear appearance by modeling the optical impulse behavior of optical fibers and improving high speed techniques. Equations also apply to fluid mechanics. This mechanic records the surface and internal dynamics of layered liquids, including rogue waves and shaft breakers. Furthermore, it contributes to understanding the interaction between atmospheric waves and improvements in climate models in meteorology. These various applications highlight the importance of the KP-mEW equation for both theoretical research and practical engineering solutions.

This nonlinear model is due to the long wavelength oceanic waves along with low intensity nonlinear restoring forces and dispersion of frequency [25,26]. Ghosh and Das studied the KP-mEW equation from the perspective of time-dependent fractional order using the (G'/G^2)-expansion technique and F expansion method [27]. The modified (G'/G^2)-expansion scheme was employed by Behera et al. [28] to construct soliton solutions of Eq (1.1). Wazwaz studied the solutions of the same equation using sine-cosine and tanh schemes [15].

It is necessary to mention the effectiveness and efficiency of the newly modified (G'/G^2)-expansion method in solving nonlinear evolution equations. The resulting solutions are plotted in different 2D and 3D plots to describe various waveforms. The obtained results look different than the results found in the literature. We have found many important studies in the literature related to this research. Using the double $(G'/G, 1/G)$-extension method, Miah et al. [29] found enormous number of closed form wave solutions of the (2+1) dimension Maccari system, Korteweg-de Vries-Burgers equation and the generalized shallow water wave equation. Haghighi and Manafian [30] used the weak-form integral equation method to examine Boussinesq-like equation comprising the β-derivative. The modified sine–Gordon equation method was used by El-Shiekh and Gaballah [31] to find a new type of solitary-wave solutions for Davey–Stewartson system and coupled nonlinear Schrödinger equations with variable coefficients. Ibrahim et al. [32] proven a new analytic technique to solve nonlinear conformable time-fractional water wave dynamical equation in complex domains using symmetric and conforming differential operators. A generalized (G'/G)-expansion scheme was used by Shallal et al. [33] to construct precise solutions of nonlinear partial differential equations in the sense of conformable fractional derivative. We have also verified the novelty of this research, and that all results suggest a great influence in the ocean engineering field by mentioning some studies published in well-known journals [15,27,28].

The focus on the complexity contains the analysis of phase portraits, chaotic patterns, multistability, and Lyapunov exponents for the KP-mEW equation. Chaotic analyses in particular are important for analyzing the nonlinear behavior and initial-condition dependence of the system [34]. Bifurcation diagrams are important tools for exploring transitions between different states, such as transitions between chaotic and periodic states. These plots not only show how the stability of the

system is maintained with the parameters but also identify the bifurcation thresholds that influence the system's future evolution.

The phenomenon of multistability recognizes several stable states and helps us to understand the role of initial conditions in the system's behavior. However, the Lyapunov exponent measures the rate of divergence between trajectories and thus provides a true measure of the stability and chaos of the system [35]. Collectively, these instruments signify a broad methodology to address the stability, chaos analysis, and sensitivity in nonlinear models across diverse fields like business, engineering, and related fields of science.

The new modified extended direct algebraic technique within the sense of confirmable fractional derivatives was utilized by Seadawy et al. [36] to research the (3+1)-dimensional fractional time-space Kadomtsev Petviashivili equation, which propagates the acoustic waves in an unmagnetized dusty plasma. A variety of recent families of hyperbolic and trigonometric solutions have been acquired in unmarried and distinct combinations, and additionally built graphically with the exceptional parametric picks. The modified extended tanh and the generalized Kudryashov techniques in the sense of a conformable fractional derivative were implemented on the (3+1)-dimensional Kadomtsev Petviashvili equation to uncover new bright, dark, periodic, horse-shoe-like, bell-shaped, and W-shaped solitary wave solutions by Hamza et al. [37].

In this paper, we have examined the KP-mEW equation from different perspectives: First, a transformation is used to transform a PDE into an ordinary differential equation. The soliton solutions are obtained by the new modified (G'/G^2)-expansion method. Additionally, 2D and 3D graphs are generated with these solutions that determine the different physical conditions of the governing model. After constructing an unperturbed dynamic system, a comprehensive investigation of the qualitative characteristics of the model is then carried out through this system. Our work contains a comprehensive investigation that comprises 2D phase portraits, chaos theory concepts, multi-stability, time series graphs, and Lyapunov exponents.

The KP-mEW model is selected in this study to explain its unique ability to describe complex nonlinear wave phenomena in multidimensional strewn systems. It combines both features of KP and modified equations of the same width (mEW) to provide a more comprehensive framework for analyzing wave expansion in oceanography, plasma physics, and optical communications than individual counterparts. The rich mathematical structure of this hybrid model, which includes high-order and nonlinearity dispersion, presents new challenges for soliton dynamics and remains physically meaningful. The aim of our research is to improve our understanding of wave interactions in real-world scenarios, to uncover new accurate solutions and stability characteristics that address the gaps in current nonlinear waveform theory, and at the same time demonstrate the effectiveness of progressive analytical methods.

This paper is organized as follows: The derived solitary wave solutions of the KP-mEW equation using the new modified (G'/G^2)-expansion method and their graphical discussion are provided first. Also, 2D and 3D graphs are given to demonstrate the physical behavior of the obtained solutions with suitable parameters. Then, we perform a bifurcation analysis of the dynamic system, followed by an investigation of quasi-periodic and chaotic behavior by adding a perturbation term in the system. A multistability analysis depending on the sets of initial conditions is then performed. Furthermore, Lyapunov exponents are utilized to analyze the sensitivity of a system to its initial conditions and to investigate the chaotic behavior of the system. Lastly, we discuss and conclude the main findings and future directions of our research.

2. Description of the new modified (G'/G^2)-expansion method

The new modified (G'/G^2)-expansion method can be expressed by some simple steps. Consider a nonlinear evolutionary equation (NLEE) as given below:

$$N\left(u, u_x, u_y, u_t, u_{xx}, u_{yy}, u_{tt}, u_{xyt}, ...\right) = 0, \tag{2.1}$$

where $u = u(x, y, t)$ is an unknown function and N is a polynomial in $u = u(x, y, t)$.

The main steps of the proposed method are given below:

Step 1: Suppose the wave variable has the following representation:

$$u(x, y, t) = U(\eta), \ \eta = Kx + Ly - Vt, \tag{2.2}$$

where V represents the wave speed, and converts Eq (2.1) into the following nonlinear ODE:

$$N\left(U, U', U'', U''', ...\right) = 0, \tag{2.3}$$

where primes denote the ordinary derivatives with respect to η. We integrate Eq (2.3) term by term one or more times, if possible.

Step 2: Suppose the formal solution of Eq (2.3) can be written as

$$U(\eta) = \alpha_0 + \sum_{i=1}^{n} \left(\alpha_i \left(H + \Theta\right)^i + \beta_i \left(H + \Theta\right)^{-i} \right), \tag{2.4}$$

where $\Theta = (G'/G^2)$, $\alpha_0, \alpha_i, \beta_i (i = 1, ..., n)$, H are unknown constants to be calculated later, and α_n, β_n cannot be zero at the same time. By considering the homogeneous balance principle between the highest-order derivative term and the highest-order nonlinear term in Eq (2.3), we can determine the degree of the positive integer n. It is supposed that Θ satisfies the Riccati equation:

$$(\Theta)' = A + C(\Theta) + B(\Theta)^2. \tag{2.5}$$

The general solutions (2.6)–(2.10) of Riccati Eq (2.5) are considered in consideration of various cases of discriminatory ability $\Delta = C^2 - 4AB$ and coefficients A, B, and C:

Case 1: For $AB > 0, C = 0,$ the solution reduces to trigonometric functions, describing periodic waves:

$$\Theta = \frac{\sqrt{AB}(P\cos(\sqrt{AB}\eta) + Q\sin(\sqrt{AB}\eta))}{A(Q\cos(\sqrt{AB}\eta) - P\sin(\sqrt{AB}\eta))}. \tag{2.6}$$

Case 2: For $AB < 0, C = 0,$ hyperbolic functions yield singular solitons:

$$\Theta = -\frac{\sqrt{|AB|}(P\sinh(2\sqrt{|AB|}\eta) + P\cosh(2\sqrt{|AB|}\eta) + Q)}{A(P\sinh(2\sqrt{|AB|}\eta) + P\cosh(2\sqrt{|AB|}\eta) - Q)}. \tag{2.7}$$

Case 3: When $A = 0, B \neq 0, C = 0,$ rational solutions obtained, modeling kink-type waves:

$$\Theta = -\frac{P}{B(P\eta + Q)}. \tag{2.8}$$

Case 4: For $C \neq 0, \Delta \geq 0,$ the solutions combine exponential/hyperbolic or trigonometric terms, capturing mixed behaviors:

$$\Theta = \frac{-C}{2B} - \frac{\sqrt{\Delta}\left(P\cosh\left(\frac{\sqrt{\Delta}}{2}\eta\right) + Q\sinh\left(\frac{\sqrt{\Delta}}{2}\eta\right)\right)}{2B\left(Q\cosh\left(\frac{\sqrt{\Delta}}{2}\eta\right) + P\sinh\left(\frac{\sqrt{\Delta}}{2}\eta\right)\right)}. \tag{2.9}$$

Case 5: For $C \neq 0, \Delta < 0,$ the solutions cartel exponential/hyperbolic or trigonometric terms, capturing mixed behaviors:

$$\Theta = \frac{-C}{2B} - \frac{\sqrt{-\Delta}\left(P\cos\left(\frac{\sqrt{-\Delta}}{2}\eta\right) - Q\sin\left(\frac{\sqrt{-\Delta}}{2}\eta\right)\right)}{2B\left(P\sin\left(\frac{\sqrt{-\Delta}}{2}\eta\right) + Q\cos\left(\frac{\sqrt{-\Delta}}{2}\eta\right)\right)}, \tag{2.10}$$

where P and Q are arbitrary constants and $\Delta = C^2 - 4AB.$

Step 3: If the degree of $U(\eta) = \mathrm{Deg}[U(\eta)] = n$, then the following formulas can be used to determine the degree of the other terms as follows:

$$\mathrm{Deg}\left[\frac{d^q U(\eta)}{d\eta^q}\right] = n + q, \mathrm{Deg}\left[(U(\eta))^p\left(\frac{d^q U(\eta)}{d\eta^q}\right)^s\right] = np + s(n+q). \tag{2.11}$$

Step 4: By plugging Eqs (2.4) and (2.5) into Eq (2.3), we derive a polynomial in $(H+\Theta)^i$, $(i = 0, \pm 1, \pm 2, ..., \pm n)$. By collecting the coefficients of the similar powers of $(H+\Theta)^i$, we can establish a set of nonlinear algebraic equations. To solve the obtained set of algebraic equations, we set each coefficient of $(H+\Theta)^i$ equal to zero, which yields a set of equations with unknown constants $\alpha_0, \alpha_n, \beta_n, a, b, r, A, B, C$, and H. The symbolic software Maple 18 is used to find the values of the unknown constants.

By putting the acquired values of the constants along with Eqs (2.6)–(2.10) into Eq (2.4), we get the precise traveling wave solution of Eq (2.1).

3. Application of the method

In order to solve the KP-mEW equation through the new modified (G'/G^2)-expansion approach, Eq (1.1) is converted into a nonlinear ordinary differential equation using Eq (2.2):

$$-K^3 bVU^{(iv)} + \left(3aK^2U^2 + rL^2 - KV\right)U'' + 6aK^2U(U')^2 = 0. \tag{3.1}$$

Integrating Eq (3.1) twice with respect to η and ignoring the constants of integration, we find

$$-K^3 bVU'' + \left(rL^2 - KV\right)U + aK^2U^3 = 0. \tag{3.2}$$

By considering the homogeneous balance between U'' and U^3 in Eq (3.2), we find the value of the positive integer n as follows: $3n = n + 2 \Rightarrow n = 1.$

Therefore, the trial solution Eq (2.4) takes the following form:

$$U(\eta)=\alpha_0+\alpha_1\left(H+\Theta\right)^1+\beta_1\left(H+\Theta\right)^{-1}. \tag{3.3}$$

Substituting Eq (3.3) along with Eq (2.5) into Eq (3.2) and equating the coefficients of $\left(H+\Theta\right)^i$ $(i=0,\pm1,\pm2,\pm3)$ to zero, we obtain a system of nonlinear algebraic equations. By solving this system with the help of Maple 18, we obtain the following solution sets.

Case 1:

$$\begin{aligned} &V=\frac{2rL^2}{K(4bABK^2-bC^2K^2+2)},\alpha_0=\frac{\sqrt{rb}L\left(C-2BH\right)}{\sqrt{a(4bABK^2-bC^2K^2+2)}},\\ &\alpha_1=\frac{2\sqrt{rb}LB}{\sqrt{a(4bABK^2-bC^2K^2+2)}},\beta_1=0,H=H,A=A,B=B,C=C. \end{aligned} \tag{3.4}$$

Case 2:

$$\begin{aligned} &V=\frac{2rL^2}{K(4bABK^2-bC^2K^2+2)},\alpha_0=\frac{\sqrt{rb}L\left(C-2BH\right)}{\sqrt{a(4bABK^2-bC^2K^2+2)}},\\ &\alpha_1=0,\beta_1=\frac{2\sqrt{rb}L(BH^2-CH+A)}{\sqrt{a(4bABK^2-bC^2K^2+2)}},H=H,A=A,B=B,C=C. \end{aligned} \tag{3.5}$$

Case 3:

$$\begin{aligned} &H=\frac{C}{2B},V=-\frac{rL^2}{K(4bABK^2-bC^2K^2-1)},\alpha_0=0,A=A,B=B,C=C,\\ &\alpha_1=\frac{i\sqrt{2rb}LB}{\sqrt{a(4bABK^2-bC^2K^2-1)}},\beta_1=\frac{i\sqrt{2rb}L(4AB-C^2)}{4\sqrt{a(4bABK^2-bC^2K^2-1)B}}. \end{aligned} \tag{3.6}$$

By substituting Eqs (3.4) and (2.6)–(2.10) into Eq (3.3), we get the following solutions:

$$\begin{aligned} u_{11}(x,y,t)=&\frac{2\sqrt{rb}LB}{\sqrt{a(4bABK^2-bC^2K^2+2)}}\left(H+\frac{\sqrt{AB}(P\cos(\sqrt{AB}\eta)+Q\sin(\sqrt{AB}\eta))}{A(Q\cos(\sqrt{AB}\eta)-P\sin(\sqrt{AB}\eta))}\right)\\ &+\frac{\sqrt{rb}L\left(C-2BH\right)}{\sqrt{a(4bABK^2-bC^2K^2+2)}}, \end{aligned} \tag{3.7}$$

$$\begin{aligned} u_{12}(x,y,t)=&\frac{2\sqrt{rb}LB}{\sqrt{a(4bABK^2-bC^2K^2+2)}}\left(H-\frac{\sqrt{|AB|}(P\sinh(2\sqrt{|AB|}\eta)+P\cosh(2\sqrt{|AB|}\eta)+Q)}{A(P\sinh(2\sqrt{|AB|}\eta)+P\cosh(2\sqrt{|AB|}\eta)-Q)}\right)\\ &+\frac{\sqrt{rb}L\left(C-2BH\right)}{\sqrt{a(4bABK^2-bC^2K^2+2)}}, \end{aligned} \tag{3.8}$$

$$u_{13}(x,y,t)=\frac{\sqrt{rb}L\left(C-2BH\right)}{\sqrt{a(4bABK^2-bC^2K^2+2)}}+\frac{2\sqrt{rb}LB}{\sqrt{a(4bABK^2-bC^2K^2+2)}}\left(H-\frac{P}{B(P\eta+Q)}\right), \tag{3.9}$$

$$u_{14}(x,y,t)=\frac{2\sqrt{rb}LB}{\sqrt{a(4bABK^2-bC^2K^2+2)}}\left(H-\frac{C}{2B}-\frac{\sqrt{\Delta}\left(P\cosh\left(\frac{\sqrt{\Delta}}{2}\eta\right)+Q\sinh\left(\frac{\sqrt{\Delta}}{2}\eta\right)\right)}{2B\left(Q\cosh\left(\frac{\sqrt{\Delta}}{2}\eta\right)+P\sinh\left(\frac{\sqrt{\Delta}}{2}\eta\right)\right)}\right)+\frac{\sqrt{rb}L(C-2BH)}{\sqrt{a(4bABK^2-bC^2K^2+2)}}, \tag{3.10}$$

$$u_{15}(x,y,t)=\frac{2\sqrt{rb}LB}{\sqrt{a(4bABK^2-bC^2K^2+2)}}\left(H-\frac{C}{2B}-\frac{\sqrt{-\Delta}\left(P\cos\left(\frac{\sqrt{-\Delta}}{2}\eta\right)-Q\sin\left(\frac{\sqrt{-\Delta}}{2}\eta\right)\right)}{2B\left(P\sin\left(\frac{\sqrt{-\Delta}}{2}\eta\right)+Q\cos\left(\frac{\sqrt{-\Delta}}{2}\eta\right)\right)}\right)+\frac{\sqrt{rb}L(C-2BH)}{\sqrt{a(4bABK^2-bC^2K^2+2)}}, \tag{3.11}$$

where $\eta=Kx+Ly-\dfrac{2rL^2}{K(4bABK^2-bC^2K^2+2)}t.$

By substituting Eqs (3.5) and (2.6)–(2.10) into Eq (3.3), we get the following solutions:

$$u_{21}(x,y,t)=\frac{2\sqrt{rb}L(BH^2-CH+A)}{\sqrt{a(4bABK^2-bC^2K^2+2)}}\left(H+\frac{\sqrt{AB}(P\cos(\sqrt{AB}\eta)+Q\sin(\sqrt{AB}\eta))}{A(Q\cos(\sqrt{AB}\eta)-P\sin(\sqrt{AB}\eta))}\right)^{-1}+\frac{\sqrt{rb}L(C-2BH)}{\sqrt{a(4bABK^2-bC^2K^2+2)}}, \tag{3.12}$$

$$u_{22}(x,y,t)=\frac{2\sqrt{rb}L(BH^2-CH+A)}{\sqrt{a(4bABK^2-bC^2K^2+2)}}\left(H-\frac{\sqrt{|AB|}(P\sinh(2\sqrt{|AB|}\eta)+P\cosh(2\sqrt{|AB|}\eta)+Q)}{A(P\sinh(2\sqrt{|AB|}\eta)+P\cosh(2\sqrt{|AB|}\eta)-Q)}\right)^{-1}+\frac{\sqrt{rb}L(C-2BH)}{\sqrt{a(4bABK^2-bC^2K^2+2)}}, \tag{3.13}$$

$$u_{23}(x,y,t)=\frac{\sqrt{rb}L(C-2BH)}{\sqrt{a(4bABK^2-bC^2K^2+2)}}+\frac{2\sqrt{rb}L(BH^2-CH+A)}{\sqrt{a(4bABK^2-bC^2K^2+2)}}\left(H-\frac{P}{B(P\eta+Q)}\right)^{-1}, \tag{3.14}$$

$$u_{24}(x,y,t)=\frac{2\sqrt{rb}L(BH^2-CH+A)}{\sqrt{a(4bABK^2-bC^2K^2+2)}}\left(H-\frac{C}{2B}-\frac{\sqrt{\Delta}\left(P\cosh\left(\frac{\sqrt{\Delta}}{2}\eta\right)+Q\sinh\left(\frac{\sqrt{\Delta}}{2}\eta\right)\right)}{2B\left(Q\cosh\left(\frac{\sqrt{\Delta}}{2}\eta\right)+P\sinh\left(\frac{\sqrt{\Delta}}{2}\eta\right)\right)}\right)^{-1}+\frac{\sqrt{rb}L(C-2BH)}{\sqrt{a(4bABK^2-bC^2K^2+2)}}, \tag{3.15}$$

$$u_{25}(x,y,t)=\frac{2\sqrt{rb}L(BH^2-CH+A)}{\sqrt{a(4bABK^2-bC^2K^2+2)}}\left(H-\frac{C}{2B}-\frac{\sqrt{-\Delta}\left(P\cos\left(\frac{\sqrt{-\Delta}}{2}\eta\right)-Q\sin\left(\frac{\sqrt{-\Delta}}{2}\eta\right)\right)}{2B\left(P\sin\left(\frac{\sqrt{-\Delta}}{2}\eta\right)+Q\cos\left(\frac{\sqrt{-\Delta}}{2}\eta\right)\right)}\right)^{-1}+\frac{\sqrt{rb}L(C-2BH)}{\sqrt{a(4bABK^2-bC^2K^2+2)}}, \tag{3.16}$$

where $\eta=Kx+Ly-\dfrac{2rL^2}{K(4bABK^2-bC^2K^2+2)}t.$

By substituting Eqs (3.6) and (2.6)–(2.10) into Eq (3.3), we get the following solutions:

$$u_{31}(x,y,t)=\frac{i\sqrt{2rb}LB}{\sqrt{a(4bABK^2-bC^2K^2-1)}}\left(\frac{C}{2B}+\frac{\sqrt{AB}(P\cos(\sqrt{AB}\eta)+Q\sin(\sqrt{AB}\eta))}{A(Q\cos(\sqrt{AB}\eta)-P\sin(\sqrt{AB}\eta))}\right)$$
$$+\frac{i\sqrt{2rb}L(4AB-C^2)}{4\sqrt{a(4bABK^2-bC^2K^2-1)B}}\left(\frac{C}{2B}+\frac{\sqrt{AB}(P\cos(\sqrt{AB}\eta)+Q\sin(\sqrt{AB}\eta))}{A(Q\cos(\sqrt{AB}\eta)-P\sin(\sqrt{AB}\eta))}\right)^{-1}, \tag{3.17}$$

$$u_{32}(x,y,t)=\frac{i\sqrt{2rb}LB}{\sqrt{a(4bABK^2-bC^2K^2-1)}}\left(\frac{C}{2B}-\frac{\sqrt{|AB|}(P\sinh(2\sqrt{|AB|}\eta)+P\cosh(2\sqrt{|AB|}\eta)+Q)}{A(P\sinh(2\sqrt{|AB|}\eta)+P\cosh(2\sqrt{|AB|}\eta)-Q)}\right)$$
$$+\frac{i\sqrt{2rb}L(4AB-C^2)}{4\sqrt{a(4bABK^2-bC^2K^2-1)B}}\left(\frac{C}{2B}-\frac{\sqrt{|AB|}(P\sinh(2\sqrt{|AB|}\eta)+P\cosh(2\sqrt{|AB|}\eta)+Q)}{A(P\sinh(2\sqrt{|AB|}\eta)+P\cosh(2\sqrt{|AB|}\eta)-Q)}\right)^{-1}, \tag{3.18}$$

$$u_{33}(x,y,t)=\frac{i\sqrt{2rb}LB}{\sqrt{a(4bABK^2-bC^2K^2-1)}}\left(\frac{C}{2B}-\frac{P}{B(P\eta+Q)}\right)$$
$$+\frac{i\sqrt{2rb}L(4AB-C^2)}{4\sqrt{a(4bABK^2-bC^2K^2-1)B}}\left(\frac{C}{2B}-\frac{P}{B(P\eta+Q)}\right)^{-1}, \tag{3.19}$$

$$u_{34}(x,y,t)=-\frac{i\sqrt{2rb}LB}{\sqrt{a(4bABK^2-bC^2K^2-1)}}\left(\frac{\sqrt{\Delta}\left(P\cosh\left(\frac{\sqrt{\Delta}}{2}\eta\right)+Q\sinh\left(\frac{\sqrt{\Delta}}{2}\eta\right)\right)}{2B\left(Q\cosh\left(\frac{\sqrt{\Delta}}{2}\eta\right)+P\sinh\left(\frac{\sqrt{\Delta}}{2}\eta\right)\right)}\right)$$
$$-\frac{i\sqrt{2rb}L(4AB-C^2)}{4\sqrt{a(4bABK^2-bC^2K^2-1)B}}\left(\frac{\sqrt{\Delta}\left(P\cosh\left(\frac{\sqrt{\Delta}}{2}\eta\right)+Q\sinh\left(\frac{\sqrt{\Delta}}{2}\eta\right)\right)}{2B\left(Q\cosh\left(\frac{\sqrt{\Delta}}{2}\eta\right)+P\sinh\left(\frac{\sqrt{\Delta}}{2}\eta\right)\right)}\right)^{-1}, \tag{3.20}$$

$$u_{35}(x,y,t)=-\frac{i\sqrt{2rb}LB}{\sqrt{a(4bABK^2-bC^2K^2-1)}}\left(\frac{\sqrt{-\Delta}\left(P\cos\left(\frac{\sqrt{-\Delta}}{2}\eta\right)-Q\sin\left(\frac{\sqrt{-\Delta}}{2}\eta\right)\right)}{2B\left(P\sin\left(\frac{\sqrt{-\Delta}}{2}\eta\right)+Q\cos\left(\frac{\sqrt{-\Delta}}{2}\eta\right)\right)}\right)$$
$$-\frac{i\sqrt{2rb}L(4AB-C^2)}{4\sqrt{a(4bABK^2-bC^2K^2-1)B}}\left(\frac{\sqrt{-\Delta}\left(P\cos\left(\frac{\sqrt{-\Delta}}{2}\eta\right)-Q\sin\left(\frac{\sqrt{-\Delta}}{2}\eta\right)\right)}{2B\left(P\sin\left(\frac{\sqrt{-\Delta}}{2}\eta\right)+Q\cos\left(\frac{\sqrt{-\Delta}}{2}\eta\right)\right)}\right)^{-1}, \tag{3.21}$$

where $\eta=Kx+Ly+\frac{rL^2}{K(4bABK^2-bC^2K^2-1)}t$.

4. Results and discussion

With the help of the new modified (G'/G^2)-expansion method, the Kadomtsev Petviashvili-modified equal width (KP-mEW) equation has been effectively solved demonstrating the kink, periodic, singular-periodic, and singular-soliton solutions. Depending on the parameter values, the traveling wave solutions can have various shapes. A variety of soliton wave solutions are generated by changing the values of the parameters A, B, P, Q, a, b, and r. It is important to highlight that the traveling wave solutions obtained for the KP-mEW equation are different and new, and more general solutions are found for particular values of the free parameters. The main advantage of the proposed

method is that it offers a number of new exact traveling wave solutions that are more universal with varying free parameters. All of the discovered solutions are original and have never been documented in the past.

The KP hierarchy is a fully integrated system and plays many important roles in the fields of mathematics and physics. The KP hierarchy has a sub-layer, that is, the B type 2 KP (MS2BKP) hierarchy, with the limit of the BKP hierarchy for the Lax operator [38]. The authors in [39] examined the integrable properties of the invariant generation functions of hop-link HOPFLY PTs colored with different representations and showed that such generation functions are functions of the KP hierarchy.

A helpful tool for discussing and outlining problem solutions in a clear and brief way is a graphical depiction. A graph is a graphic representation of quantitative, qualitative, or other commonly contrasted solutions or data. We need to have a basic understanding of graphs in order to execute computations. There are several parameters in these solutions. Because the parameters affect how the solution is shaped, we can input arbitrary values for the parameters to produce a wide range of graphs. We can identify the type of solitons using the graphs. Figures 1–9 display some of the acquired findings in 3D and 2D graphs.

Figure 1 represents the periodic soliton solution, described by a repeating pattern with sharp and regular peaks for the values of parameters $A = 1$, $B = 1$, $P = 1$, $Q = 1$, $K = 1$, $a = 1$, $b = 1$, and $r = 1$ of Eq (3.7). The 2D graph verifies the oscillatory periodic behavior. In Figure 2, 3D and 2D graphs represent the singular periodic soliton solution for the values of parameters $A = 1$, $B = -1/4$, $P = 1$, $Q = 2$, $K = 1$, $a = 1$, $b = -1$, and $r = 1$ of Eq (3.8). The 3D plot depicts the periodicity together with singular peaks at some points and the 2D plot verifies this singular behavior. Figure 3 represents the smooth and localized transitions forming a kink soliton solution for the values of parameters $A = 3$, $B = 1$, $P = 2$, $Q = 4$, $K = 1$, $a = -3$, $b = 2$, and $r = 5$ of Eq (3.10). The 3D plot shows the smooth transition between two states, forming a kink shape, and the 2D plot confirms this shape without singular behavior. Figure 4 represents the uniform periodicity forming a periodic soliton solution for the values of parameters $A = 1$, $B = 2$, $P = 2$, $Q = 3$, $K = 1$, $a = 3$, $b = 2$, and $r = 5$ of Eq (3.11). In Figure 5, 3D and 2D graphs represent the singular periodic soliton solution for the values of parameters $A = 1$, $B = 1$, $P = 1$, $Q = -4$, $K = -1$, $a = 1$, $b = 1$, and $r = 1$ of Eq (3.12). The 3D plot depicts the periodic peaks but with shifted symmetry. Figure 6 represents the singular kink soliton solution for the values of parameters $A = 0$, $B = 1$, $P = 1$, $Q = 1$, $K = 1$, $a = -1$, $b = 1$, and $r = 1$ of Eq (3.14). In Figure 7, 3D and 2D graphs represent the singular periodic-kink soliton solution for the values of parameters $A = 1$, $B = 2$, $P = 1$, $Q = 2$, $K = 1$, $a = 2$, $b = 2$, and $r = 2$ of Eq (3.16). The 3D plot depicts the localized periodic patterns with singular appearances. Figure 8 represents the localized irregular patterns forming the singular periodic-kink soliton solution for the values of parameters $A = 1$, $B = 1$, $P = 1$, $Q = 1$, $K = 1/2$, $a = -1$, $b = 1$, and $r = 1$ of Eq (3.17). Figure 9 represents the regular, constrained oscillation forming periodic soliton solution for the values of parameters $A = 2$, $B = 1$, $P = 1$, $Q = 1$, $K = 1/2$, $a = 1$, $b = 1$, and $r = -1$ of Eq (3.21).

The advantages and disadvantages of the present method are: The proposed method creates a variety of accurate solutions based on the free parameters of the auxiliary Riccati equation, providing more flexibility than limiting methods such as the tanh function and exp function methods. It avoids complex transformations or powerful symbolic calculations. This means that higher orders of nonlinear PDEs are more likely to be resolved faster and easier than some iterative or perturbation-based approaches. It works well with a variety of nonlinear evolutionary equations (NLEEs), including those with mixed dispersion and nonlinearity. The proposed method depends heavily on the selection of the appropriate parameters for the auxiliary equation. Wrong choices can lead to trivial or redundant solutions. The proposed method combats severe conjugation or multidimensional PDEs, where

methods such as Hirotas could be more effective or reversed. Simpler methods such as the tanh function require careful handling of the uniform homogeneous principles that are both troublesome in strong nonlinearity or higher-order equations.

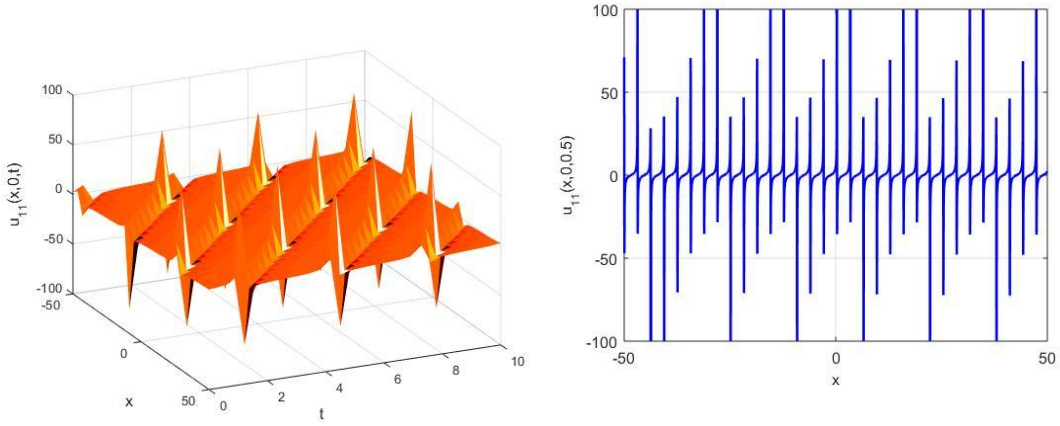

Figure 1. 3*D* and 2*D* graphs for $u_{11}(x,y,t)$.

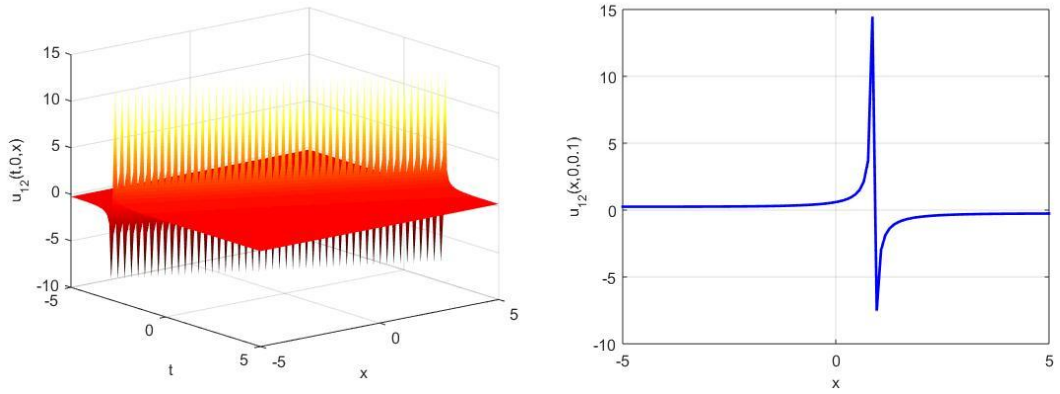

Figure 2. 3*D* and 2*D* graphs for $u_{12}(x,y,t)$.

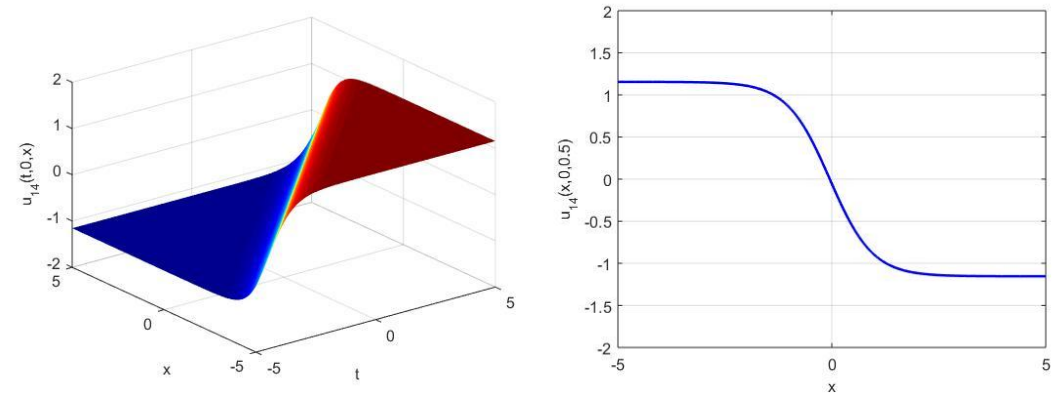

Figure 3. 3*D* and 2*D* graphs for $u_{14}(x,y,t)$.

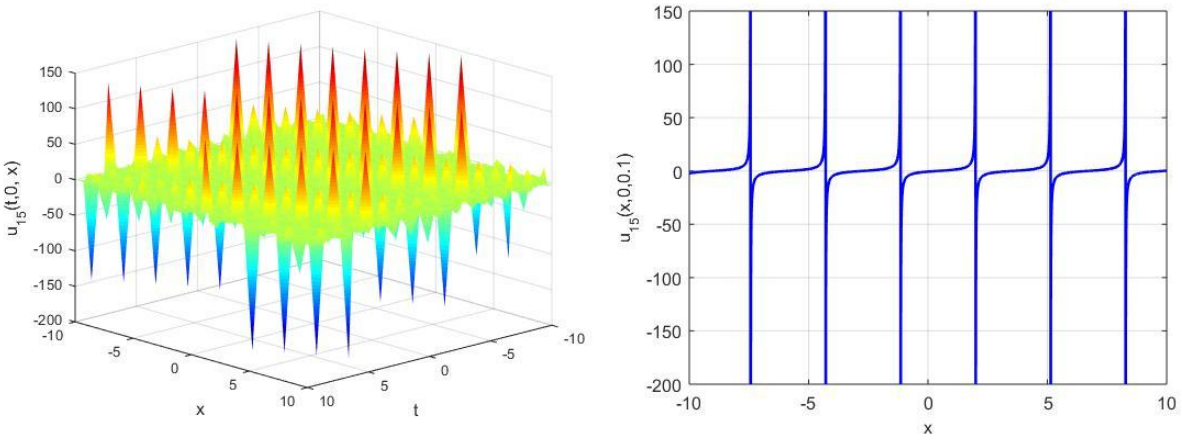

Figure 4. 3*D* and 2*D* graphs for $u_{15}(x, y, t)$.

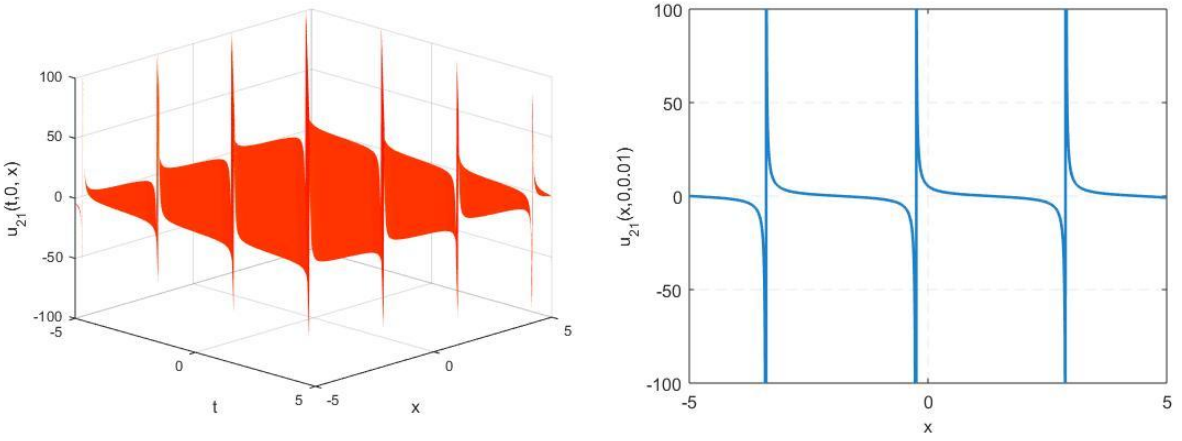

Figure 5. 3*D* and 2*D* graphs for $u_{21}(x, y, t)$.

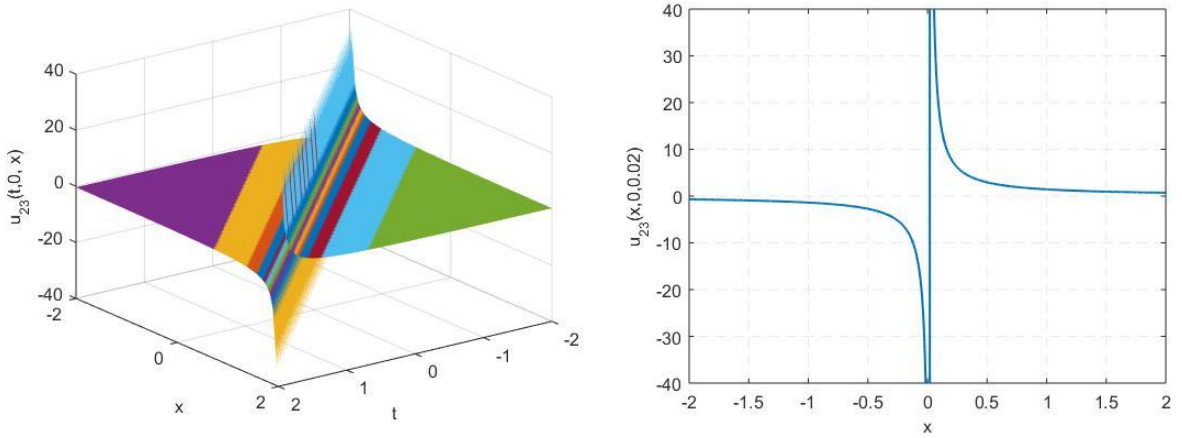

Figure 6. 3*D* and 2*D* graphs for $u_{23}(x, y, t)$.

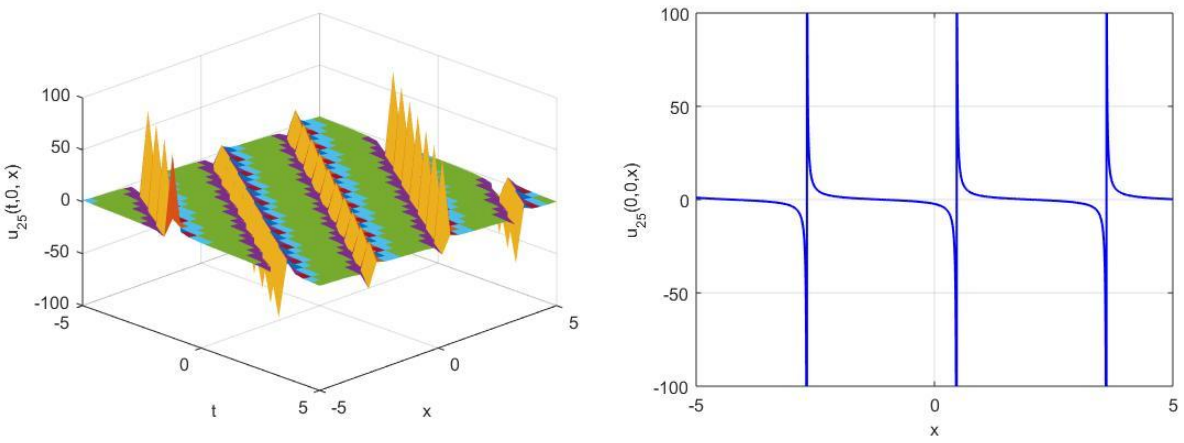

Figure 7. 3*D* and 2*D* graphs for $u_{25}(x, y, t)$.

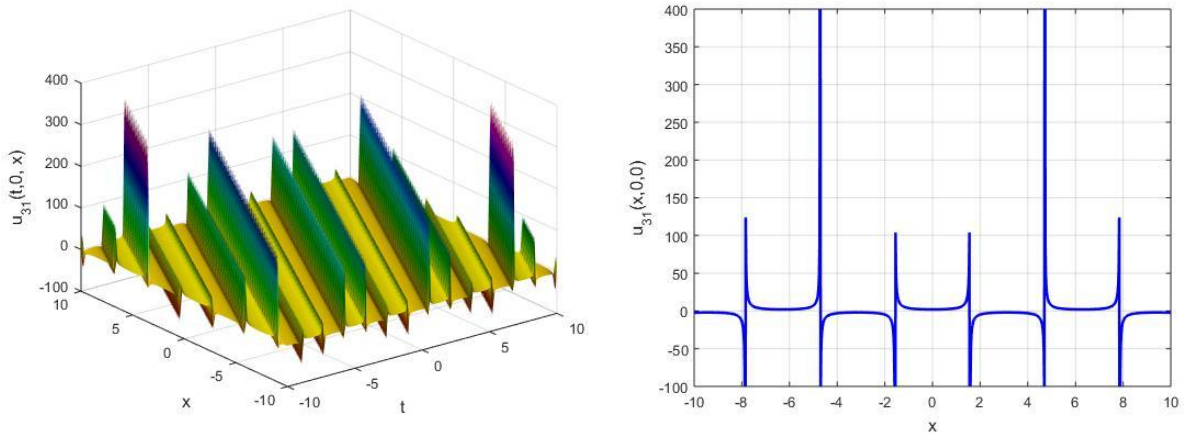

Figure 8. 3*D* and 2*D* graphs for $u_{31}(x, y, t)$.

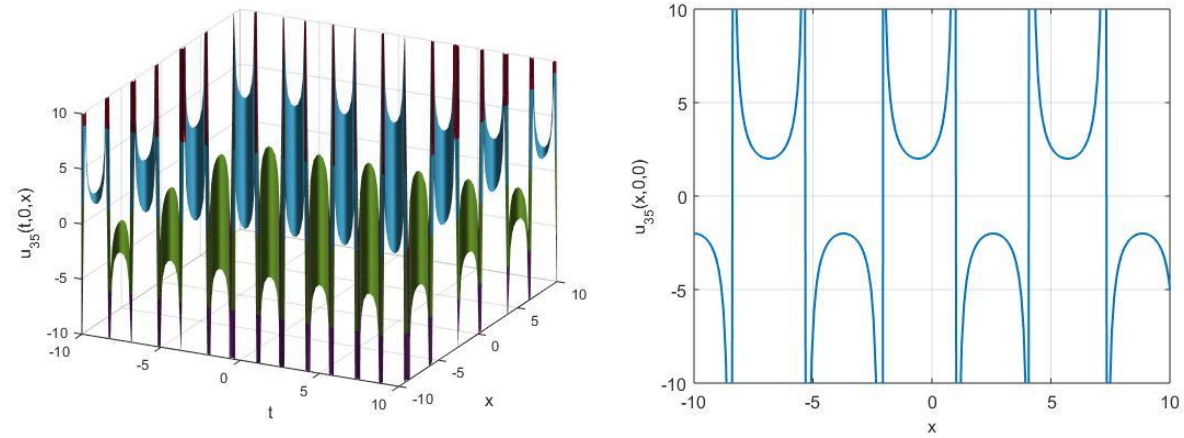

Figure 9. 3*D* and 2*D* graphs for $u_{35}(x, y, t)$.

The novel modified (G'/G^2)-expansion method significantly promotes the traditional (G'/G)-expansion method by introducing a nonlinear auxiliary equation with improved parametric flexibility.

This innovation allows for the derivation of previously inaccessible solutions, such as singular period waves, hybrid solitons, and simultaneous computational efficiency. This method is characterized by powerful nonlinear systems, particularly the KP-mEW equation, providing a more comprehensive solution. However, its effectiveness depends on carefully selecting parameters to avoid redundant solutions. These advantages provide superior analysis of fluid dynamics and complex wave phenomena in physics.

Table 1 shows the comparison of our obtained solutions using the new modified (G'/G^2)-expansion method and the solutions obtained by Islam et al. [40] using the improved auxiliary equation method. We have compared only a few solutions for the sake of ease, and are in full agreement with the solutions obtained by [40].

Table 1. Comparison of our solutions and the solutions by Islam et al. [40].

Our solutions	Solutions obtained by Islam et al. [40]
If we put $K=1, L=1, H=0, a=1, b=1, r=1, A=2,$ $B=1, C=2, P=0, V=w,$ and $u_{15}(\eta)=u_1(\xi)$ in Eq (3.11), then $u_1(\xi)=-\frac{\sqrt{6}}{3}\tan(\xi).$	If we put $l=1, m=1, k=1, p=2, r=1, q=2, d_0=-1,$ and $d_1=0$ in Eq (3.1.6), then $u_1(\xi)=-\frac{\sqrt{6}}{3}\tan(\xi).$
If we put $K=1, L=1, H=0, a=1, b=1, r=1, A=2,$ $B=1, C=2, Q=0, V=w,$ and $u_{15}(\eta)=u_2(\xi)$ in Eq (3.11), then $u_2(\xi)=\frac{\sqrt{6}}{3}\cot(\xi).$	If we put $l=1, m=1, k=1, p=2, r=1, q=2, d_0=-1,$ and $d_1=0$ in Eq (3.1.7), then $u_2(\xi)=\frac{\sqrt{6}}{3}\cot(\xi).$
If we put $K=1, L=1, H=0, a=1, b=-1, r=-1, A=2,$ $B=1, C=3, P=0, V=w,$ and $u_{14}(\eta)=u_3(\xi)$ in Eq (3.10), then $u_3(\xi)=-\frac{1}{\sqrt{3}}\tanh\left(\frac{1}{2}\xi\right).$	If we put $l=1, m=-1, k=-1, p=2, q=3, r=1, d_0=1,$ and $d_1=0$ in Eq (3.1.8), then $u_3(\xi)=-\frac{1}{\sqrt{3}}\tanh\left(\frac{1}{2}\xi\right).$
If we put $K=1, L=1, H=0, a=1, b=-2, r=-2, A=2,$ $B=1, C=3, Q=0, V=w,$ and $u_{14}(\eta)=u_4(\xi)$ in Eq (3.10), then $u_4(\xi)=-\coth\left(\frac{1}{2}\xi\right).$	If we put $l=1, m=-2, k=-2, p=2, q=3, r=1, d_0=1,$ and $d_1=0$ in Eq (3.1.8), then $u_4(\xi)=-\coth\left(\frac{1}{2}\xi\right).$
If we put $K=1, L=1, H=0, a=1, b=-1, r=-1, A=-1,$ $B=1, C=2, P=0, V=w,$ and $u_{14}(\eta)=u_7(\xi)$ in Eq (3.10), then $u_7(\xi)=-\frac{2}{\sqrt{5}}\tanh\left(\sqrt{2}\xi\right).$	If we put $l=1, m=-1, k=-1, p=-1, q=2, r=1,$ $d_0=-1,$ and $d_1=0$ in Eq (3.1.12), then $u_7(\xi)=-\frac{2}{\sqrt{5}}\tanh\left(\sqrt{2}\xi\right).$
If we put $K=1, L=1, H=0, a=1, b=-1, r=-1, A=0.5,$ $B=-0.5, C=1, Q=0, V=w,$ and $u_{14}(\eta)=u_8(\xi)$ in Eq (3.10), then $u_8(\xi)=-\frac{1}{\sqrt{2}}\coth\left(\frac{1}{\sqrt{2}}\xi\right).$	If we put $l=1, m=-1, k=-1, p=0.5, q=2, r=-0.5,$ $d_0=-1,$ and $d_1=0$ in Eq (3.1.13), then $u_8(\xi)=-\frac{1}{\sqrt{2}}\coth\left(\frac{1}{\sqrt{2}}\xi\right).$

5. Bifurcation analysis

Regardless of whether the parameters are dependent on one another or not, bifurcation analysis looks at dynamical systems and observes how the system behaves at different parameter values. The observed second-order differential equation (3.2) may be transformed into two first-order differential equations by applying the Galilean transformation [41]:

$$\begin{cases} \dfrac{du}{d\eta} = v \\ \dfrac{dv}{d\eta} = F_1 u + F_2 u^3, \end{cases} \tag{5.1}$$

where $F_1 = -\frac{\left(rL^2 - KV\right)}{bVK^3}$ and $F_2 = \frac{aK^2}{bVK^3}$. The equilibrium points of dynamic system (5.1) are (0,0) and $\left(\pm\sqrt{\frac{F_1}{F_2}}, 0\right)$ provide $rL^2 - KV < 0$. Once we have the fixed points, we can analyze the stability of these points by computing the Jacobian matrix of the system (5.1). It is given by:

$$J(u,v) = \begin{vmatrix} 0 & 1 \\ F_1 + 3F_2u^2 & 0 \end{vmatrix} = F_1 + 3F_2u^2. \tag{5.2}$$

The Jacobian gives a linear approximation of the system near the fixed or equilibrium points and helps classify these points as saddle points or center points based on the eigenvalues. This analysis is fundamental in understanding the local stability of a dynamical system.

Case 1: $b > 0$, $r > 0$. In Figure 10(a), the trajectories are closed periodic orbits centered on a stable equilibrium point (center point at (0, 0)). There is no separatrices or saddle behavior present. The system exhibits purely center-like dynamics where all trajectories are periodic. Small perturbations around the equilibrium result in oscillations that do not decay or grow. This configuration is typically governed by purely conservative forces, with no damping or unstable effects.

Case 2: $b > 0$, $r < 0$. A double-lobed structure appears with trajectories forming two distinct regions connected by a separatrix as depicted in Figure 10(b). A saddle point divides the regions, while the center is still present. The system exhibits mixed dynamics, periodic orbits near the center, and trajectories tending toward the saddle. The presence of the saddle point and separatrix suggests instability for certain trajectories. For perturbations close to the saddle point, trajectories diverge along the unstable manifold, leading to splitting behavior.

Case 3: $b < 0$, $r < 0$. The trajectories form double loops around two unstable center points as shown in Figure 10(c). The center point is no longer stable, and all trajectories diverge away from the center or saddle points. The phase space is dominated by unstable dynamics. Both the center and saddle points act as sources of instability. The system exhibits outward divergence, and no periodic orbits are observed.

Case 4: $b < 0$, $r > 0$. It can be observed in Figure 10(d) that the trajectories form elongated ovals around a stable center point, with some symmetry. The system retains periodic orbits, but they are stretched along one axis, indicating anisotropy or directional bias. Stable center dynamics dominate, but the directionality suggests non-isotropic forces or interactions. The system might exhibit stronger restoring forces in one direction compared to the other.

Case 5: $b = r$. Figure 10(e) represents that the trajectories form uniform nested closed loops, centered on the equilibrium point (0, 0). No saddle points or separatrices are present, and the phase space is fully occupied by periodic orbits. The equality of parameters *b* and *r* suggests balanced conservative

dynamics. This configuration represents a purely oscillatory system with uniform dynamics and no instability. The summary of the above discussed cases in Section 5 is described below in Table 2.

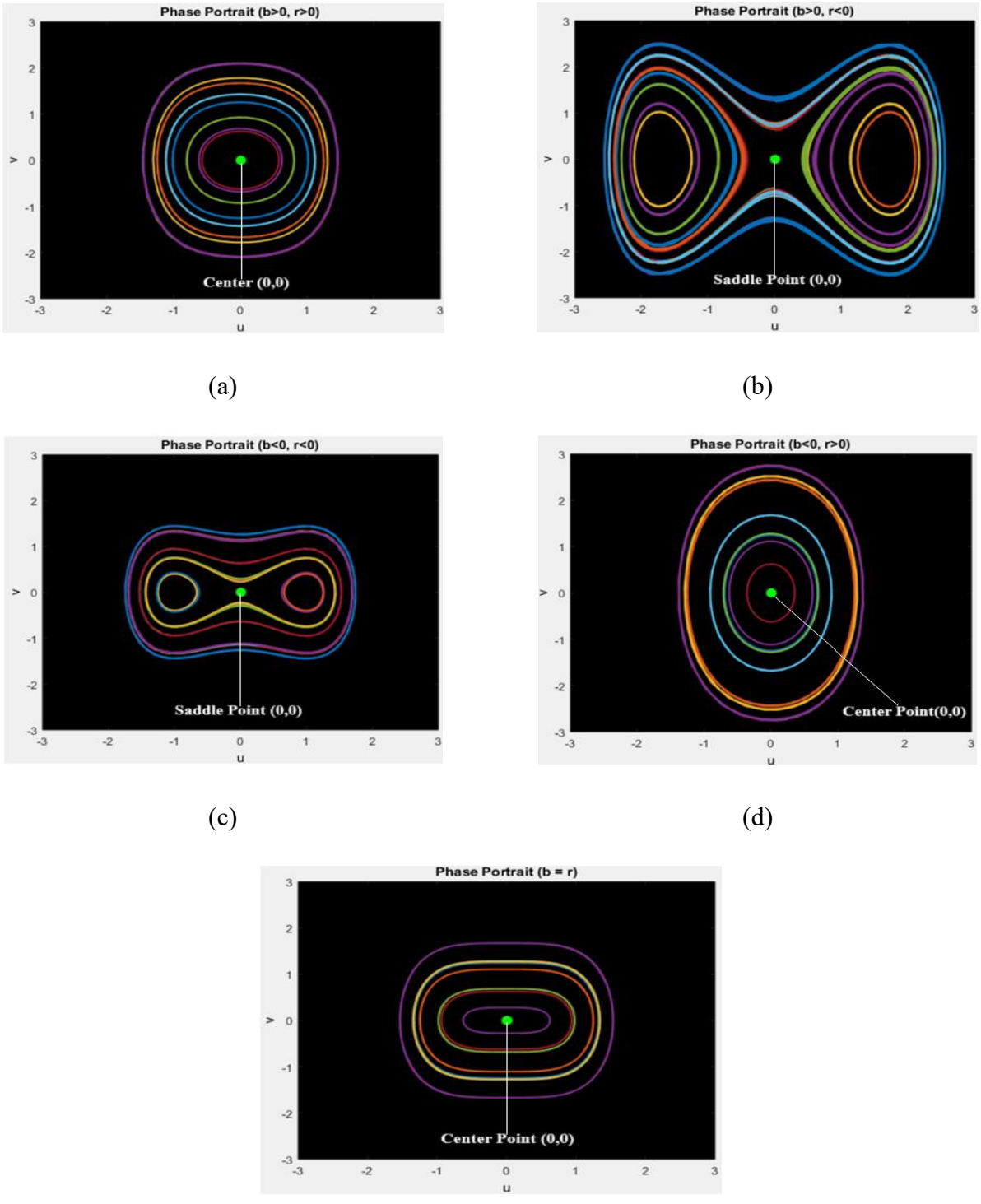

Figure 10. Phase portraits showing system dynamics for different cases.

Table 2. Summary table of cases.

Case	Conditions	Observations	System Behavior
1	$b > 0, r > 0$	Uniform periodic orbits around the center	Stable center dynamics
2	$b > 0, r < 0$	Double-lobed structure with separatrices	Mixed dynamics with saddle behavior
3	$b < 0, r < 0$	Diverging trajectories, no stable regions	Fully unstable dynamics
4	$b < 0, r > 0$	Elongated periodic orbits	Anisotropic stable dynamics
5	$b = r$	Uniform nested closed loops	Perfectly balanced oscillations

6. Chaotic analysis

In this section, we add an external force in the dynamical system (5.1) to make it perturbed as shown below:

$$\begin{cases} \dfrac{du}{d\eta} = v \\ \dfrac{dv}{d\eta} = F_1 u + F_2 u^3 + \rho\cos(\tau\eta), \end{cases} \tag{6.1}$$

where $\rho\cos(\tau\eta)$ is known as the perturbation term. In our system of equations, τ represents the frequency of the external perturbation, determining how often the external force oscillates over time, while ρ is the amplitude of the perturbation, controlling the strength of the external force [41]. The term $\rho\cos(\tau)$ models this periodic forcing. A higher τ means faster oscillations, and a larger ρ means a stronger force. Together, they define the nature of the perturbation, with stronger and more frequent forces potentially driving the system toward more complex or chaotic behavior, while weaker or slower perturbations tend to produce smoother, more regular dynamics [42].

Figure 11 demonstrates the dynamics of a nonlinear, bounded system under periodic forcing. The 2D phase portrait illustrates quasi-periodic or chaotic behavior, with knitting loops signifying sensitivity to initial conditions. The time series plot displays steady amplitude oscillations, indicating periodic or quasi-periodic behavior due to perturbation. The 3D phase portrait depicts an oscillating trajectory, emphasizing the bounded nature of the system and the interaction between velocity, displacement, and time. These plots together recommend that the system behaves like a nonlinear oscillator effected by damping and periodic forcing, maintaining stability while showing rich, complex dynamics.

The plots in Figure 12 show a nonlinear, bounded system by periodic external perturbation. The 2D phase portrait displays quasi-periodic behavior with overlapping trajectories. On the other hand, the time series plot emphasizes the nonlinearity and sensitivity in displacement over time. The 3D phase portrait provides a comprehensive evolution view of the system, verifying its stability and complex patterns. This behavior is typical of a nonlinear oscillator working in a quasi-periodic behavior.

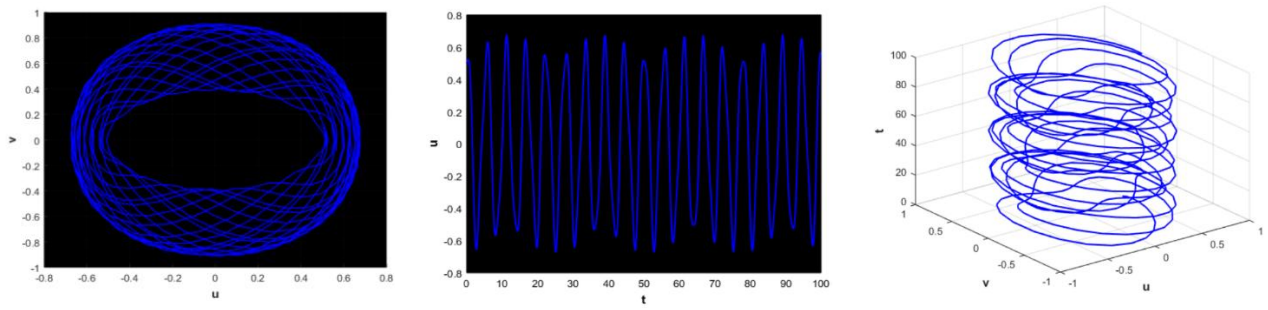

(a) (b) (c)

Figure 11. Chaotic analysis of the dynamic system: (a) 2*D* phase portrait, (b) time series analysis, and (c) 3*D* phase portrait.

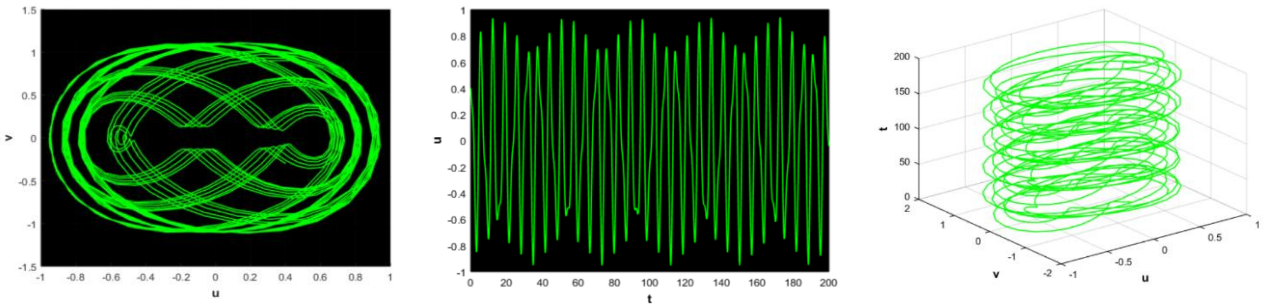

(a) (b) (c)

Figure 12. Chaotic analysis of the dynamic system: (a) 2*D* phase portrait, (b) time series analysis, and (c) 3*D* phase portrait.

7. Multistability

"Multistability" refers to the presence of multiple stable states or behavior that a dynamical system can exhibit under the same set of system parameters. It shows that the system can settle into different long-term behavior depending on its initial conditions. In a multistable system, different trajectories can lead to periodic, quasi-periodic, or chaotic outcomes, even though the system's parameters remain unchanged. This phenomenon highlights how sensitive the system is to initial conditions, where small variations in starting points can result in vastly different dynamics [43,44].

In practical terms, multistability is important because it indicates that the system can respond to perturbations or initial differences in a variety of ways, revealing complex underlying structures like attractors. It is commonly observed in systems like biological processes, climate dynamics, and mechanical systems, where different operational modes can coexist.

The plots shown in Figure 13 demonstrate the multistability of the perturbed system through both phase-space curves and time-series illustrations for three different initial conditions such that initial condition [0.10, -0.60] is shown in purple, initial condition [-0.10, 0.20] is given in green, and initial condition [0.20, -0.10] is presented in orange. In Figure 13(a), the multistability plot, the system

displays separate, overlapping periodic attractors. These attractors illuminate the sensitivity of the behavior of the system to initial conditions which is an important factor of multistability. In Figure 13(b), the time-series plot strengthens this analysis, showing periodic oscillations for all three initial conditions. Remarkably, the frequency of oscillations seems stable on all initial conditions, showing the effect of the external perturbation. Collectively, the plots confirm that the system transitions from steady state to stable periodic attractors, whose nature depends on the initial conditions, indicating predictable and non-chaotic behavior.

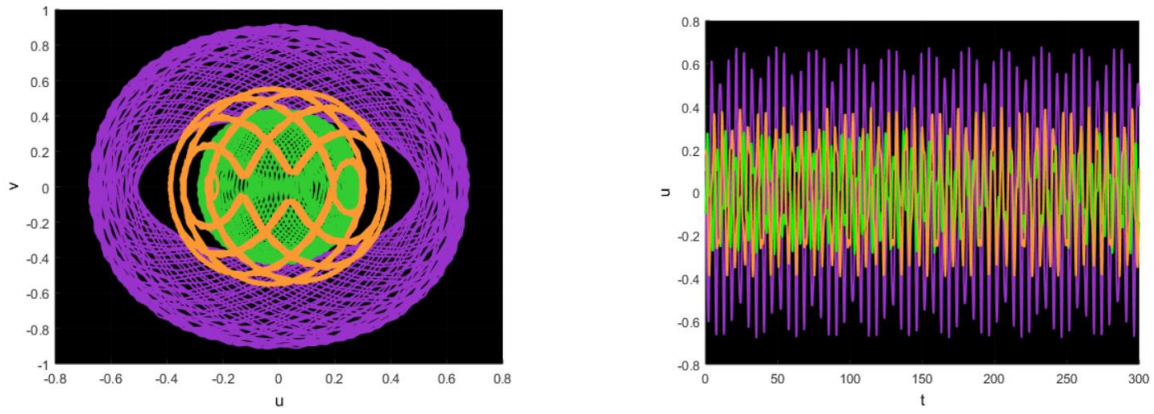

(a) (b)

Figure 13. Multistability analysis for the perturbed system (6.1) at different initial conditions.

8. Lyapunov exponents

Lyapunov exponents are utilized to analyze the sensitivity of a system to its initial conditions by evaluating the rate of convergence or divergence of adjacent trajectories in phase portraits. A positive Lyapunov exponent demonstrates chaotic conduct, where small perturbations develop exponentially over time, whereas a negative exponent recommends steadiness, stability, or convergence to a fixed point or periodic trajectory. These exponents are basic for recognizing and characterizing chaos, stability, and consistency in nonlinear dynamical systems [45].

The x-axis of the plot represents the normalized time (τ), and the y-axis Lyapunov exponent (λ) is displayed in bits/unit time. Nearly zero stabilization ($\lambda_1 \approx -0.0036$, $\lambda_2 \approx +0.0037$) indicates weak chaos, which is characteristic of disturbed systems that induce energy. This agreement observed quasi-periodic behavior and limited plasma in the marine case [44]. Numerical verification ensures reliability by confirming that these are physical effects and artifacts and Wolf methods with convergence tests [45].

Figure 14 examines the chaotic behavior of the system (6.1) with $\rho = 0.1$, $\omega = 0.5$, and initial conditions set to [0.2, -0.1] using Lyapunov exponents. At first, λ_1 and λ_2 show non-steady-state oscillations, reflecting the sensitivity of the system to initial conditions. With time, the exponents become stable to the values approximately equal but opposite, i.e., $\lambda_1 = -0.0036$ and $\lambda_2 = 0.0037$. This balance indicates limited chaotic behavior, where trajectories stay bounded within a specific region while showing exponential divergence in at least one direction, as shown by the positive value of λ_2. The negative λ_1 approves the convergence of the system in another direction, keeping its nature bounded. These outcomes confirm that the chaotic dynamics of the system, dependent on initial conditions and bounded trajectories, align with the properties of a chaotic attractor.

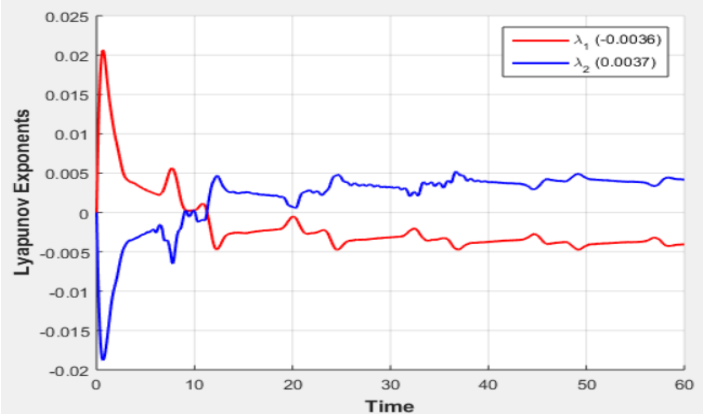

Figure 14. Investigating chaotic behavior in system (6.1) using the Lyapunov exponent chaos detection technique for $\rho = 0.1$, $\omega = 0.5$, and initial condition [0.2, -0.1].

9. Conclusions

This study successfully examined the KP-mEW equation through analytical and dynamic approaches, providing some important results. First, the new modified (G'/G^2)-expansion method produced several new accurate solutions that demonstrate superior skills compared to traditional methods, such as kink, periodic, singular periodic, and singular kink-soliton solutions. Second, comprehensive divergence analysis resulted in five different dynamic systems ranging from stable periodic orbits to completely confusing behavior determined by variations in parameters. Third, chaos analysis by disturbance identified quasi-periodic patterns and limited chaos by the Lyapunov index ($\lambda_1 = -0.0036$, $\lambda_2 = 0.0037$). These results promote nonlinear wave theory using potential applications for tsunami modeling and plasma wave expansion. Future work will need to examine experimental validation and extension of these solutions for machine learning.

Author contributions

Amna Mumtaz: Writing – original draft, Conceptualization. Muhammad Shakeel: Software, Resources. Abdul Manan: Methodology, Investigation, Formal analysis. Marouan Kouki: Visualization, Validation, Resources. Nehad Ali Shah: Writing – review and editing, Validation. All authors have read and approved the final version of the manuscript for publication.

Use of Generative-AI tools declaration

The authors declare they have not used Artificial Intelligence (AI) tools in the creation of this article.

Acknowledgments

The authors extend their appreciation to the Deanship of Scientific Research at Northern Border University, Arar, KSA, for funding this research work through the project number NBU-FPEJ-2025-2570-03.

Conflict of interest

The authors declare no conflicts of interest.

References

1. A. M. Wazwaz, *Partial differential equations and solitary waves theory*, 1 Ed., Beijing and Springer-Verlag Berlin Heidelberg, Higher Education Press, 2009.
2. Y. Ma, X. Geng, A coupled nonlinear Schrödinger type equation and its explicit solutions, *Chaos Soliton. Fract.*, **42** (2009), 2949–2953. https://doi.org/10.1016/j.chaos.2009.04.037
3. X. Yong, J. Gao, Z. Zhang, Singularity analysis and explicit solutions of a new coupled nonlinear Schrödinger type equation, *Commun. Nonlinear Sci. Numer. Simul.*, **16** (2011), 2513–2518. https://doi.org/10.1016/j.cnsns.2010.09.025
4. M. A. Akbar, N. H. M. Ali, M. T. Islam, Multiple closed form solutions to some fractional order nonlinear evolution equations in physics and plasma physics, *AIMS Math.*, **4** (2019), 397–411. https://doi.org/10.3934/math.2019.3.397
5. B. Kopcasiz, A. R. Seadawy, E. Yasar, Highly dispersive optical soliton molecules to dual-mode nonlinear Schrödinger wave equation in cubic law media, *Opt. Quant. Elect.*, **54** (2022), 194. https://doi.org/10.1007/s11082-022-03561-7
6. M. Shakeel, N. A. Shah, J. D. Chung, Novel analytical technique to find closed form solutions of time fractional partial differential equations, *Fractal Fract.*, **6** (2022), 24. https://doi.org/10.3390/fractalfract6010024
7. M. Shakeel, M. A. Iqbal, Q. Din, Q. M. Hassan, K. Ayub, New exact solutions for coupled nonlinear system of ion sound and Langmuir waves, *Indian J. Phys.*, **94** (2020), 885–894. https://doi.org/10.1007/s12648-019-01522-7
8. K. Ayub, M. Saeed, M. Ashraf, M. Yaqub, Q. M. Hassan, Soliton solutions of variant Boussinesq Equations through exp-function method, *UW J. Sci. Tech.*, **1** (2017), 24–30. https://uwjst.org.pk/index.php/uwjst/article/view/6
9. M. Shakeel, S. T. Mohyud-Din, M. A. Iqbal, Closed form solutions for coupled nonlinear Maccari system, *Comput. Math. Appl*., **76** (2018), 799–809. https://doi.org/10.1016/j.camwa.2018.05.020
10. A. Ali, A. R. Seadawy, Dispersive soliton solutions for shallow water wave system and modified Benjamin-Bona-Mahony equations via applications of mathematical methods, *J. Ocean Eng. Sci.*, **6** (2021), 85–98. https://doi.org/10.1016/j.joes.2020.06.001
11. W. Malfliet, The tanh method: a tool for solving certain classes of nonlinear evolution and wave equations, *J. Comput. Appl. Math.*, **164-165** (2004), 529–541. https://doi.org/10.1016/S0377-0427(03)00645-9
12. L. Akinyemi, U. Akpan, P. Veeresha, H. Rezazadeh, M. Inc, Computational techniques to study the dynamics of generalized unstable nonlinear Schrödinger equation, *J. Ocean Eng. Sci.*, 2022. https://doi.org/10.1016/j.joes.2022.02.011
13. A. H. Arnous, M. M. Mirzazadeh, L. Akinyemi, A. Akbulut, New solitary waves and exact solutions for the fifth-order nonlinear wave equation using two integration techniques, *J. Ocean Eng. Sci.*, **8** (2023), 475–480. https://doi.org/10.1016/j.joes.2022.02.012
14. J. Manafian, M. Lakestani, The classification of the single traveling wave solutions to the modified Fornberg–Whitham equation, *Int. J. Appl. Comput. Math.*, **3** (2016), 3241–3252. https://doi.org/10.1007/s40819-016-0288-y

15. A. M. Wazwaz, The tanh method and the sine–cosine method for solving the KP-MEW equation, *Int. J. Comput. Math.*, **82** (2005), 235–246. https://doi.org/10.1080/00207160412331296706
16. H. Yépez-Martínez, J. F. Gómez-Aguilar, A. Atangana, First integral method for non-linear differential equations with conformable derivative, *Math. Model. Nat. Phenom.*, **13** (2018), 14. https://doi.org/10.1051/mmnp/2018012
17. B. Alshahrani, H. A. Yakout, M. M. A. Khater, A. H. Abdel-Aty, E. E. Mahmoud, D. Baleanu, et al., Accurate novel explicit complex wave solutions of the (2+1)-dimensional Chiral nonlinear Schrödinger equation, *Res. Phys.*, **23** (2021), 104019. https://doi.org/10.1016/j.rinp.2021.104019
18. S. El-Ganaini, M. O. Al-Amr, New abundant solitary wave structures for a variety of some nonlinear models of surface wave propagation with their geometric interpretations, *Math. Meth. App. Sci.*, **45** (2022), 7200–7226. https://doi.org/10.1002/mma.8232
19. E. Az-Zo'bi, M. O. Al-Amr, A. Yildrim, W. A. Alzoubi, Revised reduced differential transform method using Adomian's polynomials with convergence analysis, *Math. Eng. Sci. Aero.*, **11** (2020), 827–840.
20. M. O. Al-Amr, H. Rezazadeh, K. K. Ali, A. Korkmazki, N1-soliton solution for Schrödinger equation with competing weakly nonlocal and parabolic law nonlinearities, *Commun. Theor. Phys.*, **72** (2020), 065503. https://doi.org/10.1088/1572-9494/ab8a12
21. L. Akinyemi, M. Inc, M. M. A. Khater, H. Rezazadeh, Dynamical behaviour of Chiral nonlinear Schrödinger equation, *Opt. Quant. Elect.*, **54** (2022), 191. https://doi.org/10.1007/s11082-022-03554-6
22. A. Mumtaz, M. Shakeel, M. Alshehri, N. A. Shah, New analytical technique for prototype closed form solutions of certain nonlinear partial differential equations, *Results Phys.*, **60** (2024), 107640. https://doi.org/10.1016/j.rinp.2024.107640
23. S. I. Zaki, Solitary wave interactions for the modified equal width equation, *Comput. Phys. Commun.*, **126** (2000), 219–231. https://doi.org/10.1016/S0010-4655(99)00471-3
24. T. Geyikli, S. B. G. Karakoc, Subdomain finite element method with quartic B-splines for the modified equal width wave equation, *Comput. Math. Math. Phys.*, **55** (2015), 410–421. https://doi.org/10.1134/S0965542515030070
25. S. Dusuel, P. Michaux, M. Remoissenet, From kinks to compacton-like kinks, *Phys. Rev. E*, **57** (1998), 2320–2326. https://doi.org/10.1103/PhysRevE.57.2320
26. W. X. Ma, Lump solutions to the Kadomtsev–Petviashvili equation, *Phys. Lett. A*, **379** (2015), 1975–1978. https://doi.org/10.1016/j.physleta.2015.06.061
27. A. Das, N. Ghosh, Bifurcation of traveling waves and exact solutions of Kadomtsev–Petviashvili modified equal width equation with fractional temporal evolution, *Comput. Appl. Math.*, **38** (2019), 9. https://doi.org/10.1007/s40314-019-0762-3
28. S. Behera, N. H. Aljahdaly, J. P. S. Virdi, On the modified $(\frac{G'}{G^2})$-expansion method for finding some analytical solutions of the traveling waves, *J. Ocean Eng. Sci.*, **7** (2022), 313–320. https://doi.org/10.1016/j.joes.2021.08.013
29. M. M. Miah, A. R. Seadawy, H. S. Ali, M. A. Akbar, Abundant closed form wave solutions to some nonlinear evolution equations in mathematical physics, *J. Ocean Engin. Sci.*, **5** (2020), 269–278. https://doi.org/10.1016/j.joes.2019.11.004
30. M. Parto-Haghighi, J. Manafian, Solving a class of boundary value problems and fractional Boussinesq-like equation with β-derivatives by fractional-order exponential trial functions, *J. Ocean Engin. Sci.*, **5** (2020), 197–204. https://doi.org/10.1016/j.joes.2019.11.003

31. R. M. El-Shiekh, M. Gaballah, Solitary wave solutions for the variable-coefficient coupled nonlinear Schrödinger equations and Davey–Stewartson system using modified sine-Gordon equation method, *J. Ocean Engin. Sci.*, **5** (2020), 180–185. https://doi.org/10.1016/j.joes.2019.10.003
32. R. W. Ibrahim, C. Meshram, S. B. Hadid, S. Momani, Analytic solutions of the generalized water wave dynamical equations based on time-space symmetric differential operator, *J. Ocean Engin. Sci.*, **5** (2020), 186–195. https://doi.org/10.1016/j.joes.2019.11.001
33. M. A. Shallal, K. K. Ali, K. R. Raslan, H. Rezazadeh, A. Bekir, Exact solutions of the conformable fractional EW and MEW equations by a new generalized expansion method, *J. Ocean Engin. Sci.*, **5** (2020), 223–229. https://doi.org/10.1016/j.joes.2019.12.004
34. A. Jhangeer, Beenish, Dynamics and wave analysis in longitudinal motion of elastic bars or fluids, *Ain Shams Eng. J.*, **15** (2024), 102907. https://doi.org/10.1016/j.asej.2024.102907
35. A. Jhangeer, A. R. Ansari, M. Imran, Beenish, M. B. Riaz, Lie symmetry analysis, and traveling wave patterns arising the model of transmission lines, *AIMS Math.*, **9** (2024), 18013–18033. https://doi.org/10.3934/math.2024878
36. A. R. Seadawy, M. Younis, M. Z. Baber, S. T. R. Rizvi, M. S. Iqbal, Diverse acoustic wave propagation to confirmable time-space fractional KP equation arising in dusty plasma, *Commun. Theor. Phys.*, **73** (2021), 115004. https://doi.org/10.1088/1572-9494/ac18bb
37. A. E. Hamza, K. S. Mohamed, A. Mustafa, K. Aldwoah, M. Hassan, H. Saber, Abundant novel stochastic fractional solitary wave solutions of a new extended (3+1)-dimensional Kadomtsev–Petviashvili equation, *Alex. Eng. J.*, **119** (2025), 45–55. https://doi.org/10.1016/j.aej.2025.01.073
38. C. Li, $N=2$ supersymmetric extension on multi-component D type Drinfeld–Sokolov hierarchy, *Phys. Lett. B*, **855** (2024), 138771. https://doi.org/10.1016/j.physletb.2024.138771
39. C. Li, A. Mironov, A. Yu. Orlov, Hopf link invariants and integrable hierarchies, *Phys. Lett. B*, **860** (2025), 139170. https://doi.org/10.1016/j.physletb.2024.139170
40. M. T. Islam, M. A. Akter, S. Ryehan, J. F. Gómez-Aguilar, M. A. Akbar, A variety of solitons on the oceans exposed by the Kadomtsev Petviashvili-modified equal width equation adopting different techniques, *J. Ocean Engin. Sci.*, **9** (2024), 566–577. https://doi.org/10.1016/j.joes.2022.07.001
41. S. N. Chow, J. K. Hale, *Methods of bifurcation theory*, Springer Science & Business Media, 1982.
42. M. B. Riaz, A. Jhangeer, F. Z. Duraihem, J. Martin, Analyzing dynamics: Lie symmetry approach to bifurcation, chaos, multistability, and solitons in extended (3+1)-dimensional wave equation, *Symmetry*, **16** (2024), 608. https://doi.org/10.3390/sym16050608
43. A. Jhangeer, Beenish, Study of magnetic fields using dynamical patterns and sensitivity analysis, *Chaos Soliton. Fract.*, **182** (2024), 114827. https://doi.org/10.1016/j.chaos.2024.114827
44. A. Jhangeer, W. Faridi, M. Alshehri, The study of phase portraits, multistability visualization, Lyapunov exponents and chaos identification of coupled nonlinear volatility and option pricing model, *Eur. Phys. J. Plus*, **139** (2024), 658. https://doi.org/10.1140/epjp/s13360-024-05435-1
45. A. Wolf, J. B. Swift, H. L. Swinney, J. A. Vastano, Determining Lyapunov exponents from a time series, *Phys. D*, **16** (1985), 285–317. https://doi.org/10.1016/0167-2789(85)90011-9